High-average-power, high-repetition-rate dual signal optical parametric oscillator based on PPMgLN

Feng Ji (纪 峰)[1,2*], Rongsheng Lu (卢荣胜)[1], Baosheng Li (李保生)[1], Baigang Zhang (张百钢)[2], and Jianquan Yao (姚建铨)[2]

[1]*School of Instrument Science and Opto-Electronics Engineering, Hefei University of Technology, Hefei 230009, China*

[2]*College of Precision Instrument and Opto-Electronics Engineering, Tianjin University, Tianjin 300072, China*

[*]*E-mail: jifengtju@163.com*

Received September 3, 2009

A high-average-power, high-repetition-rate dual signal optical parametric oscillator based on periodically poled MgO-doped lithium niobate (PPMgLN) with a phase-reversed grating is reported. The pump laser is an acousto-optically Q-switched Nd:YVO_4 laser with a maximum average power of 7.6 W. When the repetition rate is 50 kHz and the pulse width of the pump source is 23 ns, the maximum average dual signal output power is about 1.9 W, leading to a conversion efficiency of 25%. Over a 30-min interval, the instability of the signal power measured is less than 0.5%.

OCIS codes: 190.2620, 190.4410, 190.4970.

doi: 10.3788/COL20100805.0505.

Quasi-phase-matching (QPM) technique has become a hotspot in nonlinear optics due to its prominent properties such as walk-off free and the access to the highest valued nonlinear coefficient[1−5]. Furthermore, the fabrication method based on the electric field poling technique permits flexible design of the QPM grating pattern[6]. Therefore, various phase-matching behaviors such as multi-wavelength second harmonic generation (SHG), third harmonic generation (THG), and dual-signal-wave (DSW) optical parametric oscillation (OPO) have been demonstrated by use of the QMP devices[7−9].

There are various patterns in non-uniform QPM gratings, such as the Fibonacci-based grating, the chirped grating, the aperiodic grating, and the periodically phase-reversed (PPR) grating[7−11]. Zhu *et al.* introduced the Fibonacci structure in the QPM grating and demonstrated THG in a single chip[7]. Chou *et al.* introduced the structure with the periodic phase reversals to demonstrate multi-wavelength phase-matching[8]. Gu *et al.* theoretically proposed aperiodically poled grating optimized by simulated annealing algorithm[11]. Lee *et al.* demonstrated multi-wavelength SHG based on aperiodic and PPR grating, respectively[12]. Comparatively speaking, the PPR grating is relatively easy to be designed. Furthermore, it is much suitable to realize multiple QPM processes with rather high Fourier coefficients for which several closely spaced effective QPM periods are needed.

A DSW OPO can be simply demonstrated by using periodically poled $LiNbO_3$ (PPLN) with a series of gratings[13]. However, in order to obtain the simultaneous oscillation of the DSWs, the focus condition of the pump laser should be carefully adjusted in the experiment. Sasaki *et al.* demonstrated a DSW OPO based on PPR-PPLN[14]. Compared to the former structure, the PPR avoided the strict adjustment of the focus location of the pump laser and provided a larger effective nonlinear coefficient under the same crystal length.

Recently, periodically poled MgO-doped $LiNbO_3$ (PPMgLN) has been regarded as a promising candidate for PPLN with a high resistance to the photorefractive damage and a low coercive field so that the PPMgLN crystal can be fabricated with a large aperture for high energy conversion and can be operated at room temperature[15].

In our previous work, we have demonstrated a DSW optical parametric generator (OPG) based on PPR-PPMgLN with a dual signal output power of 410 mW at a 10-kHz repetition rate[16]. In this letter, we present a high-repetition-rate, high-average-power operation of a DSW PPR-PPMgLN OPO. As high as 1.9-W DSW power with 50-kHz repetition rate is obtained.

In the first order QPM interaction, the wave-vector mismatch is given by

$$\Delta k_{\rm Q} = 2\pi\left(\frac{n_{\rm p}}{\lambda_{\rm p}} - \frac{n_{\rm s}}{\lambda_{\rm s}} - \frac{n_{\rm i}}{\lambda_{\rm i}} - \frac{1}{\Lambda_0}\right), \tag{1}$$

where λ is the wavelength, n is the refractive index, the subscripts p, s, and i represent the pump, signal, and idler waves, respectively; Λ_0 is the grating period. Multiple QPM processes can be realized if the uniform QPM grating is superimposed by a phase reversal sequence with a grating period $\Lambda_{\rm ph}$ at the same time as the following equation is satisfied:

$$\Delta k_Q = \frac{2k\pi}{\Lambda_{\rm ph}}, \tag{2}$$

where k is an integer number and $\Lambda_{\rm ph}$ is referred to as phase-reversed period.

Here we expect to realize DSW OPO operation using this type of QPM structure, so we choose k as 1 and –1 and thus we can obtain

$$\frac{n_{\rm p}}{\lambda_{\rm p}} - \frac{n_{\rm s_1}}{\lambda_{\rm s_1}} - \frac{n_{\rm i_1}}{\lambda_{\rm i_1}} - \frac{1}{\Lambda_0} - \frac{1}{\Lambda_{\rm ph}} = 0, \tag{3}$$

$$\frac{n_{\rm p}}{\lambda_{\rm p}} - \frac{n_{\rm s_2}}{\lambda_{\rm s_2}} - \frac{n_{\rm i_2}}{\lambda_{\rm i_2}} - \frac{1}{\Lambda_0} + \frac{1}{\Lambda_{\rm ph}} = 0. \tag{4}$$

The nonlinear material was selected to be MgO-doped $LiNbO_3$ and the refractive index was provided by HC

 © 2010 Chinese Optics Letters

Photonics Corp. We chose the QPM grating period and phase-reversed period as 29.6 μm and 6.8 mm, respectively. The total crystal length was 47.6 mm. In order to estimate the single pass amplifier coefficient based on this crystal as a function of the signal wavelength, we adopted the transfer matrix method as reported in Ref. [17]. Using Eqs. (4)–(6) in Ref. [17], the amplifier coefficient as a function of the signal wavelength can be calculated, as shown in Fig. 1 (crystal temperature: 30 °C; pump wavelength: 1064 nm; pump intensity: 1×10^{11} W/m^2). There are two strong expected signal peaks at 1473.2 and 1487.7 nm, and the theoretical single-pass linewidths are 0.9 and 1.1 nm, respectively. Besides the two strong expected peaks, there are several unwanted small sidebands, which can be regarded as noises. From the figure we can see that the noise-signal ratio is less than 5%. Compared to the SHG, this ratio is much smaller[12]. This is because the SHG conversion efficiency is proportional to the square of the nonlinear coefficient, whereas the OPO amplifier coefficient has an exponential relationship with the square of the nonlinear coefficient. These sidebands in the OPO spectrum are significantly suppressed. In the experiments, the sidebands will be further suppressed, sometimes even eliminated since the amplifier coefficients at these sidebands are too small to reach the OPO threshold, so we just observe DSWs in the measured spectrum. Using the same method, we also obtain dual-signal peaks of 1487.7 and 1504.4 nm at 100 °C, 1518.8 and 1540.4 nm at 200 °C.

We also employ the Fourier expansion method to obtain the Fourier coefficients for these two QPM processes. These values are 0.404 and 0.408 while the theoretical maximal value of the ideal uniform periodic grating structure is $2/\pi = 0.6366$.

A schematic diagram of the DSW OPO setup is shown in Fig. 2. The pump laser used in our experiment was a 1064-nm diode-pumped Nd:YVO_4 laser (Aion Industrial-V, Bavarian, Germany). Operating in the acousto-optically Q-switched mode, its repetition rate

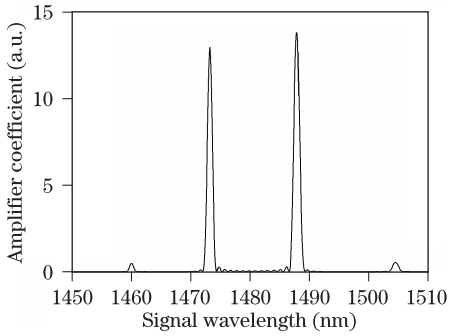

Fig. 1. Theoretically calculated dual-signal spectrum. Crystal temperature: 30 °C; pump wavelength: 1064 nm; pump intensity: 1×10^{11} W/m^2.

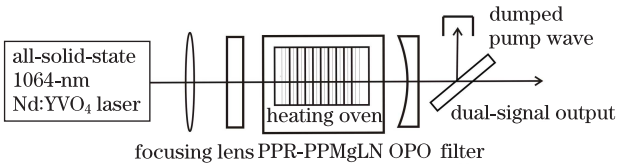

Fig. 2. Experimental setup.

could be tuned in the range of 1–100 kHz. In the experiment, the repetition rate of the pump source was fixed at 50 kHz. The maximum average pump power was 7.6 W. The laser mode was TEM_{00} with beam quality factor $M^2 < 1.3$. The pulse width decreased with the diode incident current increasing and was about 23 ns at the maximum output. The laser beam was focused to a 44-μm spot (radius) at the center of the PPR-PPMgLN crystal by a single 100-mm-focal-length lens. The input mirror of the OPO cavity was plano and had > 95% transmissivity at 1064 nm, 99% reflectivity at the signal wavelength from 1470 to 1540 nm. The output mirror had a radius of curvature of 100 mm and transmissivities of 86% at 1064 nm and 14%–16% at the signal wavelength. The two mirrors absorbed idler wave in the range of 3–4 μm by the glass substrates. The plano-concave cavity was separated by 86 mm, giving a waist of 65 μm for an optimally mode-matched pump. The distance between the focusing lens and the input mirror was about 82 mm. Both end faces of the PPR-PPMgLN crystal were antireflection (AR) coated with reflectivities of less than 1%, 1%, and 3% for the pump, signal, and idler wavelengths, respectively. The PPR-PPMgLN crystal was placed in an oven which permitted varying the temperature with an accuracy of 0.1 °C from room temperature up to 200 °C. The polarization of the pump laser was parallel to the z-axis of the PPR-PPMgLN crystal for the first-order QPM with the nonlinear coefficient d_{33}. A dichromatic filter was used to block the pump wave so as to measure the highly transmitted dual-signal power. A Molectron EPM1000 power meter was used to measure the powers of the pump wave and the DSW.

Figure 3 shows the average dual-signal power as a function of the 1064-nm pump power at different crystal temperatures. In the experiment, firstly, we find that the dual-signal output power increased with the crystal temperature increasing. At the maximum pump power of 7.6 W, dual-signal powers of 0.9, 1.3, and 1.9 W are obtained at 30, 100, and 200 °C, respectively. This is partly because the transmissivity of the output mirror increases with the signal wavelength increasing, which is good for the signal power coupling out. Secondly, the parametric gain is enhanced with the temperature increasing. Furthermore, the transmissivity of the signal and idler waves in the crystal is an increasing function of the crystal temperature. The oscillation threshold almost has no change while the temperature varies. Over the range of 30–200 °C, the thresholds are all about 1.8 W. At the threshold, the pump pulse width is about 35 ns, so the corresponding threshold pump intensity is 27 MW/cm^2. At a pump power of 6.4 W, we have measured the power stability. Over a 30-min interval, the instability of the dual signal output power is found to be about 0.5% (root-mean-square (RMS)). In the measurements, the PPR-PPMgLN crystal is kept at 200 °C.

An Agilent 86142B optical spectrum analyzer was used to measure the dual-signal spectra, which are shown in Fig. 4. DSWs of 1474.6 and 1488.9 nm at 30 °C, 1488.7 and 1504.9 nm at 100 °C, 1517.7 nm and 1538.4 nm at 200 °C are achieved, respectively. The linewidths of the signal waves are all about 0.4 nm. From the figure we can see that the intensity at the long signal wavelength is a little lower than that at the short one, which does

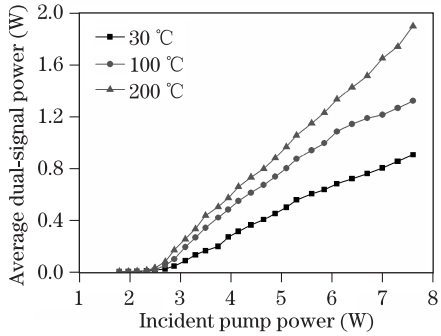

Fig. 3. Dependence of the average dual-signal power on the 1064-nm pump power.

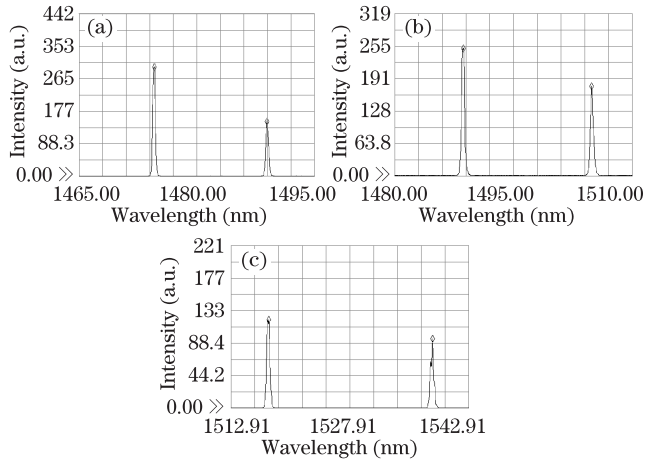

Fig. 4. Dual-signal spectra at (a) 30, (b) 100, and (c) 200 °C.

not agree with the theoretical prediction. The discrepancy may be attributed partly to the accuracy of the crystal refractive index and the control precision of the temperature controller, partly to the fabrication errors. We also find that with the temperature increasing, the intensity differences between the dual-signal radiations reduces. This may be attributed to the same reason for the power increase with the temperature increasing.

In conclusion, we have demonstrated a high-average-power, high-repetition-rate DSW OPO based on PPR-PPMgLN pumped by a Q-switched Nd:YVO_4 laser. The average dual-signal output power of 1.9 W with 25% conversion efficiency is achieved. Over a 30-min interval, the instability of the two idler output power is found to be about 0.5% (RMS). The DSWs with spacing of several nanometers may be well suited for some potential applications such as differential absorption lidar (DIAL), differential precision laser spectroscopy, and differential frequency generation of terahertz (THz) waves[9,13−15].

This work was supported in part by the National Natural Science Foundation of China (No. 50875074), the Program for Innovative Research Team of Hefei University of Technology, the Key Project of Chinese Ministry of Education (No. 108073), and the Doctoral Special Supporting Foundation of Hefei University of Technology (No. GDBJ2008-026).

References

1. B. Zhang, J. Yao, X. Ding, H. Zhang, P. Wang, D. Xu, G. Yu, and F. Zhang, Chin. Phys. **13,** 0364 (2004).
2. J. Yang, X. Li, J. Yao, and P. Bing, Chinese J. Lasers (in Chinese) **35,** 1459 (2008).
3. F. Ji, B. Zhang, E. Li, H. Li, R. Zhou, T. Zhang, P. Wang, and J. Yao, Opt. Commun. **262,** 234 (2006).
4. F. Ji, J. Yao, B. Zhang, T. Zhang, D. Xu, and P. Wang, Chin. Phys. B **17,** 1286 (2008).
5. Y. Peng, Y. Lu, G. Xie, W. Wang, and D. Wu, Chinese J. Lasers (in Chinese) **35,** 670 (2008).
6. L. Myers, R. Eckardt, M. Fejer, R. Byer, W. Bosenberg, and J. Pierce, J. Opt. Soc. Am. B **12,** 2102 (1995).
7. S. Zhu, Y. Zhu, and N. Ming, Science **278,** 843 (1997).
8. M. Chou, K. Parameswaran, M. Fejer, and I. Brener, Opt. Lett. **24,** 1157 (1999).
9. K. Kawase, T. Hatanaka, H. Takahashi, K. Nakamura, T. Taniuchi, and H. Ito, Opt. Lett. **25,** 1714 (2000).
10. M. Arbore, O. Marco, and M. Fejer, Opt. Lett. **22,** 865 (1997).
11. B. Gu, B. Dong, Y. Zhang, and G. Yang, Appl. Phys. Lett. **75,** 2175 (1999).
12. Y. Lee, F. Fan, Y. Huang, B. Gu, B. Dong, and M. Chou, Opt. Lett. **27,** 2191 (2002).
13. T. Hatanaka, K. Nakamura, T. Taniuchi, and H. Ito, Electron. Lett. **36,** 1409 (2000).
14. Y. Sasaki, A. Yuri, K. Kawase, and H. Ito, Appl. Phys. Lett. **81,** 3323 (2002).
15. H. Ishizuki and T. Taira, Opt. Lett. **30,** 2918 (2005).
16. F. Ji, X. Li, B. Zhang, T. Zhang, P. Wang, D. Xu, and J. Yao, Chin. Phys. Lett. **24,** 3157 (2007).
17. Y. Zhang and B. Y. Gu, Opt. Commun. **192,** 417 (2001).